Oscillation of the Fe and Co Magnetic Moments near the Sharp (1 −1 0) Fe/Co Interface

B. Swinnen, J. Meersschaut, J. Dekoster, G. Langouche, S. Cottenier, S. Demuynck, and M. Rots
Instituut voor Kern- en Stralingsfysica, K. U. Leuven, Celestijnenlaan 200 D, B-3001 Leuven, Belgium
(Received 4 March 1996)

By means of high resolution time differential perturbed angular correlation spectroscopy on diamagnetic Cd incorporated into MBE-grown Fe/Co multilayers, we accurately determine the transferred magnetic hyperfine fields in the layers. We assign experimentally observed satellite fields to probes in plateaus near a sharp interface. These fields are used to fit magnetic moments near the Fe/Co interface. We obtain a moment profile that oscillates with the layer number in both Fe and Co near the sharp (1 −1 0) Fe/Co interface. [S0031-9007(96)02174-6]

PACS numbers: 75.70.Cn, 75.50.Cc, 76.80.+y

In the past few years much effort has been devoted to the study of hyperfine fields and magnetic moments at and near surfaces and interfaces. For 3D transition metals, theory predicts a strong moment enhancement at clean surfaces and at interfaces with noble metal substrates, while interaction with nonmagnetic transition metal substrates reduces ferromagnetism [1]. Only a few experimental techniques have the necessary spatial resolution to probe interface magnetism. Gradmann and co-workers used conversion electron mossbauer spectroscopy to probe Fe surfaces, near surface layers and buried interfaces [2]. Other groups used magnetic circular x-ray dichroism or magnetization measurements to investigate interfaces and to extract information about the averaged moments at the interface [3,4]. We use perturbed angular correlation (PAC) spectroscopy [5] to study the hyperfine fields in Fe/Co superlattices, and we link the measured hyperfine fields to a microscopic model for the magnetic moments in each layer near the Fe/Co interface.

The samples reported on are molecular-beam epitaxy (MBE) grown under the same conditions as in [6]. They are of the form (1 −1 0)-GaAs/Fe 200 Å/$(\mathrm{Co/Fe})_{10}$ with a Co thickness of 20 Å and Fe thicknesses of 10, 25, and 40 Å. As in [7], we monitored the quality of the lattice during growth with reflection high energy electron diffraction, and after growth we checked the multilayer structure with x-ray diffraction (XRD). For the PAC experiment we implanted trace amounts of 80 keV ^{111}In atoms (probes) into the multilayers. Ions are stopped in the bulk of the layers as well as near the interfaces: Individual monolayers are not populated selectively. A PAC experiment results in a time dependent anisotropy ratio $R(t)$ which is obtained as described in [6]. $R(t)$ typically is a superposition of periodic components, each characteristic of one probe environment. For pure magnetic interactions those components contain a Larmor frequency together with its second harmonic. It is proportional to the hyperfine field characteristic of the probe's site. The orientation of the hyperfine field relative to the detectors determines the relative amplitude of the harmonics.

Our PAC setup consists of two independent spectrometers incorporated into each other, as in Fig. 1. For a single magnetic hyperfine field orientation, we simultaneously take spectra with the magnetic hyperfine field at 45° between the detectors [Fig. 1(a), horizontal plane] and perpendicular to the detector plane [Fig. 1(a), vertical plane]. In the first case, one only observes first harmonics; in the second case, only second harmonics occur. When the field is as in Fig. 1(b), one finds a constant partial spectrum for the horizontal plane when using only the detectors that are aligned with the hyperfine field as a start for the coincidence measurement. With this field orientation the spectrum obtained from the vertical setup has equal amplitudes for both harmonics. With these field-detector geometries, one easily confirms that in our samples all hyperfine fields are along the [1 1 0] axis in the plane of the multilayer.

Figure 2 shows room-temperature $R(t)$ spectra for one of the multilayers together with a fit to the data. Similar spectra were taken on all samples at various temperatures. The inset in Fig. 2(a) shows the Fourier transform (FT) of an experimental curve. Since the FT is calculated from a finite time domain (400 ns), it only gives an idea of the frequency components of the experimental $R(t)$ ratio. The $R(t)$ itself, however, is the interference pattern of all present frequencies. It is a complex signal of which the apparent period and amplitude may vary with time. Its frequency content is found by *fitting* it to well known theoretical curves *in time domain.* When, as in the experiments below, a large number of periods is available in the $R(t)$ spectrum, then the fit is extremely sensitive

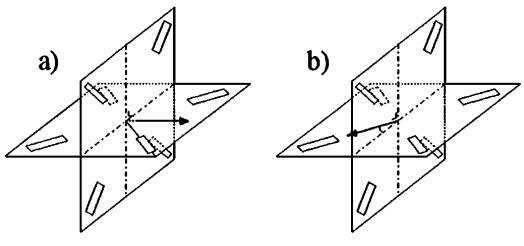

FIG. 1. Schematic drawing of the double PAC spectrometer. Four detectors are at 90° angle with each other both in a vertical and a horizontal plane. The arrow shows the special hyperfine field orientations (a) and (b) relative to the detectors.

 0031-9007/97/78(2)/362(4)$10.00

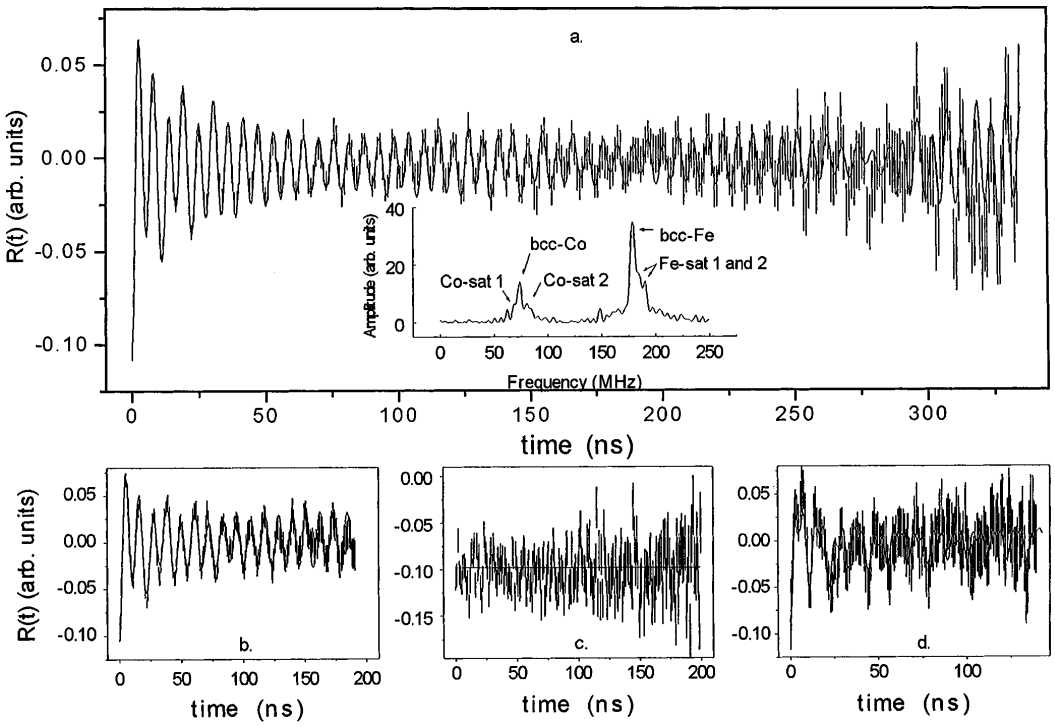

FIG. 2. TDPAC spectra as taken on one of the multilayers (Fe 40 Å). The data points are at the centers of the displayed error bars. (a) Field geometry as in Fig. 1(a) vertical plane: All hyperfine fields are perpendicular to the detector plane. A Fourier transform of experimental data is shown in the inset. (b) Field geometry as in Fig. 1(a) horizontal plane. (c) Field geometry as in Fig. 1(b) horizontal plane; partial spectrum with start detector aligned with the hyperfine field. (d) Field geometry as in Fig. 1(b) vertical plane.

to small field shifts. Hence we determined field values from spectra as the one in Fig. 2(a), where only second harmonics occur by fitting the experimental spectra to

$$R(t) = A_{22}^{\text{eff}} \sum_{i=1}^{n} f_i^* (\cos 2\nu_L^i t)^* \ \exp\left(-\frac{1}{2}\sigma_i^2 t^2\right).$$

The effective anisotropy A_{22}^{eff} for our setup is -0.12, n is the number of probe sites, f_i is the relative fraction of site i, and σ_i is proportional to the width of the Gaussian distribution on the Larmor frequency ν_L^i characteristic of site i. Spectra taken for other field geometries as the ones in Fig. 2(b), 2(c), and 2(d) are used to cross check the fit results.

In the final fit model, each spectrum is fitted with eight purely magnetic probe sites. It is the simplest model that accounts for all the $R(t)$ spectra (36) taken on the different samples in a consistent way. Omitting one component results in misfits that occur systematically in the different spectra. Alternatively, one may try replacing one or more components by a combined magnetic dipole and electric quadrupole interaction. Although, under such assumptions, reasonable fits are obtained for a single spectrum, the spectra taken in complementary field geometries cannot be fit consistently. Hence combined interactions do not occur in the spectra, and the fit model is unique [8].

We calculated the room temperature mean values of the hff at the different probe sites listed in Table I using a g factor of -0.306 for ^{111}Cd. For the thinnest sample, 75% of the probes (60% for the thickest one) is found in the broad field distributions Δ_{Co} and Δ_{Fe}. These cause the fast decay of the anisotropy curve's amplitude in the first 50 ns of Fig. 2(a) but do not contribute beyond this point. They result from many microscopically slightly different probe environments. Since the mean fields of these distributions are between the ones for Cd in bulk Fe and bcc Co and because their fractions are proportional to the interface density ($1/\Lambda$, with Λ the bilayer thickness), we assign them to probe atoms in a mixed FeCo environment at a *diffuse interface.* Two other contributions, undoubtedly from their hff, originate from probes in pure bcc Fe and pure bcc Co [6], and for each of them we find two additional satellite fields. These latter six fields are sharply defined (for these sites $\sigma_i = 0$): The amplitude of the $R(t)$ in Fig. 2(a) does not decay between 50 and 300 ns, thus excluding a spread on the field values. The beating in this part of the spectrum allows one to resolve the satellite

TABLE I. Experimental magnetic hyperfine fields (B_{hf}) and their Lorentzian distributions (δ) for the different probe sites.

Structure	Bhf (T)	δ (%)	Structure	Bhf (T)	δ (%)
bcc Co	16.13(6)	⋯	bcc Fe	38.11(3)	⋯
Co sat I	15.6(1)	⋯	Fe sat I	38.7(2)	⋯
Co sat II	17.2(2)	⋯	Fe sat II	39.8(3)	⋯
Δ_{Co}	18.7(7)	8.7(7)	Δ_{Fe}	36.(4)	21.(1)

fields even though their fractions are of the order of 5%–10% only. The satellite fields are reproducible within 1%. For the CdFe and CdCo fields, the reproducibility is better than 0.5%. The satellites correspond to bcc Fe or bcc Co alike configurations. Since there is no distribution or quadrupole interaction on these fields, they cannot result from the diffuse interface or from step positions at a sharp interface or from defect sites. (A cubic defect as the one in [9] is improbable for bcc structures and would involve a larger field shift relative to the bulk CdFe and CdCo fields.) Therefore the satellite fields are assigned to probe atoms either in Fe or in Co layers in plateaus near a *sharp interface.* A well defined interface is also evidenced by the XRD experiments, clearly reflecting the bilayer period as shown in [7]. Finally, it is possible that, due to radiation damage, a limited fraction of the probes ended up in ill-defined defect sites. These may contribute to the missing fraction ($\pm 10\%$) or to the large frequency distributions Δ_{Fe} and Δ_{Co}.

The experiments thus evidence a structure model including both diffuse and sharp interfaces. When the multilayer is grown, first a bcc-Fe buffer of good crystal quality is deposited. It is a well documented fact that the Co deposited on top of this buffer layer, grows pseudomorphically on Fe in a bcc phase up to a thickness of 10 Å. Beyond this thickness, Co grows in a mixed fcc-hcp structure. Only when Fe is deposited on top of the Co is the upper part of the layer forced back into a bcc structure [7]. Because of the lattice mismatch between the two phases, resulting in many defects in the mixed fcc-hcp structure, this phase transition is likely to be induced by interdiffusion of the Fe into the Co, creating a mixed FeCo phase. This growth model explains the coexistence of both sharp (Co on Fe) and diffuse interfaces (Fe on Co) in one sample, as shown in Fig. 3, eventually consistent with the ^{59}Co NMR work by Panissod *et al.* [10]. We stress that the sharp interface is not necessarily flat: The experiments indicate only that plateaus are large enough to allow for well defined hyperfine fields.

We use the Stearns model for the hff [11] to implement our experimental field values. Within this model the transferred hyperfine field (B_{hf}) at a diamagnetic probe as ^{111}Cd is the sum of a negative term due to the $4s$ conduction electron polarization at the probe site (B_Σ) and a term with opposite sign due to the shielding of the excess charge by the valence s electrons near the probe atom (B_v):

$$B_{\mathrm{hf}} = B_\Sigma + B_v \, .$$

Here B_Σ is the sum over the field contributions ΔB_i at the probe site induced by atoms i of the surrounding lattice. The field shift induced per Bohr magneton of the polarizing atom ($\Delta B_i/\mu_B$) depends on the distance between the probe and polarizing atom, hence its shell number (n) relative to the probe. The moment of the polarizing atom, however, depends on its layer number (L) relative to the interface. Table II lists, for the 5 *nn* shells around the probe atom in a (1 −1 0) oriented bcc lattice, the number of atoms that are found in the Lth layer above (below) the one containing the probe atom. Using this table we can, for any given moment configuration at the Fe/Co interface, calculate B_Σ at the Cd probe in any layer near the sharp interface as

$$B_\Sigma = \sum_i \frac{\Delta B_{n(i)}}{\mu_B} \; * \; \mu_{L(i)} \, ,$$

where the first factor is determined by the shell number of the polarizing atom relative to the probe, and the second by the number, relative to the interface, of the layer in which the polarizing atom is contained. In practice, one calculates B_Σ by summing over the first few nearest neighbor (*nn*) shells.

We calculated the $\Delta B_n/\mu_B$ values in Table II from field-shift values in [6] and [11] through rescaling to Cd-probe atoms [11] and normalization to the magnetic moments of bulk Fe and Co, respectively. For Cd in Fe we calculate B_v by subtracting B_Σ for Cd in bulk Fe from the total hff known from experiment, $B_v^{\mathrm{Fe}} = 9.6$ T. For Cd in Co the estimated value from [6], $B_v^{\mathrm{Co}} = 14.5$ T, is used. We recall that B_v is determined mainly by the atoms in the first *nn* shell which, for a (1 −1 0) bcc lattice, only has atoms in the layer of the probe and in its

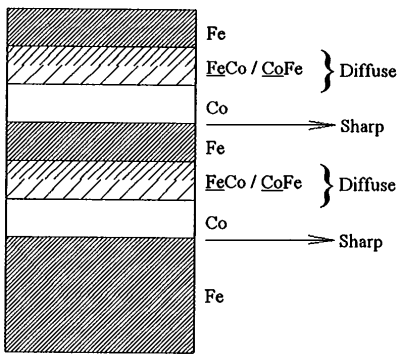

FIG. 3. Model for the structure of the Fe/Co multilayer as derived from the present data.

TABLE II. Number of neighbors as a function of the layer number (L) relative to the layer of the probe and as a function of the nearest neighbor shell number (n). Conduction electron polarization contributions to the hyperfine field in Tesla per atom and per μ_B for Cd in Fe and in Co as functions of the shell number.

			Probe			Fe	Co
L	−II	−I	0	I	II	$\Delta B_n/\mu_B$	$\Delta B_n/\mu_B$
n						(T/μ_B)	(T/μ_B)
1		2	4	2		−3.94	−2.71
2		2	2	2		−0.89	−1.69
3	1	4	2	4	1	0.79	0.55
4	4	6	4	6	4	0.20	0.38
5	2		4		2	0.10	−0.32

adjacent layers. Therefore we only need a new estimate of B_v for the first Fe and Co layer at the interface. A first approximation is made by normalizing the B_v for Fe and Co to the number of Fe and Co *nn*. This yields $B_v = 10.8$ T for Cd in the first Fe layer and $B_v = 13.3$ T for Cd in the first Co layer at the interface.

With this model and the available data on the 5 *nn* atomic shells, we fit magnetic moment profiles in Fe and Co near the sharp interface. Starting from a configuration in which all Fe and Co layers have the bulk moment, $2.20\mu_B$ for Fe and $1.65\mu_B$ for Co, we calculate B_{hf} for six layers at both sides of the interface. We define χ^2 as the sum of the squared differences between the calculated fields and the closest experimental field. Consequently, χ^2 is minimized by varying one or more moments near the interface. This was done for all configurations with less than six free moments near the interface. We find a pronounced minimum for χ^2 by varying three moments in Fe and two moments in Co, consistent with the interpretation by Pizzini *et al.* [3] of older magnetization experiments. We remark that the field of Fe satellite I (Table I) was not found in our fit. Instead, the field for Cd in bulk Fe was fitted for the first and third Fe layer at the interface. For the model to distinguish between these two, it would have to be accurate within 1%, which is beyond the precision of the hff model. The resulting magnetic moment profile of Fig. 4 shows that moments oscillate with the layer number. We find an average moment for the three Fe layers at the interface of $2.4\mu_B$. The average moment over the five perturbed layers is $2.1\mu_B$ which is 20% smaller than the value reported in [3]. While here we probe the sharp interface separately, magnetization experiments probe the entire superlattice. In the alloyed region of the diffuse interface, the Fe and Co moments can be considerably enhanced ($3\mu_B$ for Fe in FeCo alloys with more than 30% Co), thus increasing the mean interface moment.

We finally comment on the restraints of our model. For bulk Co we used a magnetic moment of $1.65\mu_B$ while, in the literature, values between $1.65\mu_B$ and $1.71\mu_B$ are found [3,12]. Although a different bulk Co moment may change the fitted Co moments near the interface by less than 10%, it does not affect the Fe moments, because these are connected to the former in second order only via the hyperfine fields in the first two Co layers. The same conclusion is drawn concerning the effect of a possible error on the $\Delta B_n/\mu_B$ values for Cd in bcc Co: Varying these estimates up to 10% caused small changes of the Co moments but again did not affect the Fe moments significantly. Only the approximation of B_v at the interface may cause deviations for the first layers at the interface, but once more will influence the other moments only indirectly. In view of these remarks, we estimate the accuracy of the fitted moments at 5% for Fe and 15% for Co.

We are grateful to Professor J. C. Soares and Dr. N. P. Barradas (CFN, Universidade de Lisboa, Portugal) for helpful collaboration in the initial stage of this work and for the benefits from the use of their analysis routine. This project was financially supported by the Belgian Concerted Action (GOA), the University Attraction Poles (UIAP), and the Interuniversitar Institute for Nuclear Sciences (IIKW) programs. J. M. is supported by the IWT Foundation, Contract No. 943054.

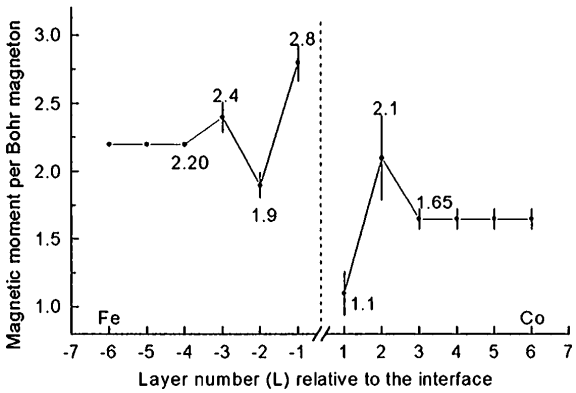

FIG. 4. Magnetic moment profile in Fe and Co near the (1 −1 0) Fe/Co interface.

[1] A. J. Freeman and Ru-qian Wu, J. Magn. Magn. Mater. **100**, 497 (1991).
[2] M. Albrecht, U. Gradmann, T. Furubayashi, and W. A. Harrison, Europhys. Lett. **20**, 65 (1992); J. Korecki and U. Gradmann, Phys. Rev. Lett. **55**, 2491 (1985); G. Liu and U. Gradmann, J. Magn. Magn. Mater. **118**, 99 (1993).
[3] S. Pizzini *et al.*, Phys. Rev. B **50**, 3779 (1994), and references therein.
[4] J. Vogel, G. Panaccione, and M. Sacchi, Phys. Rev. B **50**, 7157 (1994).
[5] For a review on the method, see Th. Wichert and E. Recknagel, in *Microscopic Methods in Metals*, edited by U. Gonser (Springer, Berlin, 1986), p. 317.
[6] B. Swinnen, J. Dekoster, G. Langouche, and M. Rots, Phys. Rev. B **52**, 5962 (1995).
[7] J. Dekoster, E. Jedryka, C. Mény, and G. Langouche, Europhys. Lett. **22**, 433 (1993).
[8] B. Swinnen, J. Dekoster, J. Meersschaut, S. Cottenier, S. Demuynck, G. Langouche, and M. Rots (to be published).
[9] C. Hohenhemser, A. R. Arends, H. De Waard, H. G. Devaere, F. Pleiter, and S. A. Drentje, Hyperfine Interact. **3**, 297 (1977); F. Raether, G. Weyer, K. P. Lieb, and J. Chevallier, Phys. Lett. A **131**, 471 (1988).
[10] P. Panissod, J. P. Jay, C. Meny, M. Wojcik, and E. Jedryka, Hyperfine Interact. **97–98**, 75 (1996).
[11] M. B. Stearns, Phys. Rev. B **8**, 4383 (1973).
[12] B. I. Min, T. Oguchi, and A. J. Freeman, Phys. Rev. B **33**, 7852 (1986); V. L. Moruzzi, P. M. Marcus, K. Schwarz, and P. Mohn, Phys. Rev. B **34**, 1784 (1986); D. J. Singh, Phys. Rev. B **45**, 2258 (1992); J. Dekoster, E. Jedryka, M. Wojcik, and G. Langouche, J. Magn. Magn. Mater. **126**, 12 (1993).